ELSEVIER

Computer Physics Communications 109 (1998) 207–226

Computer Physics Communications

Monte Carlo optimization applied to symmetry breaking

Jai Sam Kim [a,1], J.C. Tolédano [b], P. Tolédano [c]

[a] *Department of Physics, Pohang University of Science and Technology, Pohang 790-784, South Korea*

[b] *École Polytechnique, Rte de Saclay, F-91128, Palaiseau, France*

[c] *Grp de Physique théorique, Faculté des Sciences, 33 rue St-Leu, F-80000, Amiens, France*

Received 1 August 1997; revised 17 November 1997

Abstract

We present a Monte Carlo optimization algorithm to search for the boundary points of the orbit space which is important in determining the symmetry breaking directions in the Higgs potential and the Landau potential. Our algorithm is robust and generally applicable. For large problems we have also developed a parallel version. We apply the method to the Landau potential of the d-wave abnormal superconductor, He-3, and a SU(5) Higgs potential. © 1998 Elsevier Science B.V.

PACS: 02.70.L; 12.10.-g; 64.60.-i; 74.20.De

PROGRAM SUMMARY

Title of program: MCMIN

Catalogue identifier: ADHM

Program obtainable from: CPC program Library, Queen's University of Belfast, N. Ireland

Licensing provisions: none

Computer for which the program is designed and others on which it has been tested: any Unix or VMS machines, the parallel version runs on Intel Paragon only

Operating systems under which the program has been tested: Unix, VMS

Programming languages used: FORTRAN 77 and C

Memory required to execute with typical data: 1500 kwords

No. of bits in a word: 32

No. of processors used: one for the sequential version, 60 for the parallel version

Has the code been vectorised?: no, but parallelised

No. of bytes in distributed program, including test data, etc.: 3182

Distribution format: ASCII

Nature of physical problem

A Monte Carlo algorithm minimizing the Higgs potential and the Landau potential. The group theoretical and geometrical method requires the orbit space which is a confined region of 'angular' space. The orbit space boundaries indicate the symmetry breaking directions. Our algorithm is robust and generally applicable. For large problems we have also developed a parallel version. We apply the method to the Landau potential of the d-wave abnormal

[1] E-mail: jsk@postech.ac.kr

PII S0010-4655(97)00139-2

superconductor, He-3, and a SU(5) Higgs potential.

Method of solution

The program initially samples orbit points and computes the center of gravity of these points. It then selects the most outward points along angular rays. Then these random walkers are allowed to make random moves and the outward movement is encouraged using the rejection method. When a random walker strays into another angular ray, its position is compared with that of incumbent random walker and the one which is more outward is selected. All rays are surveyed and the procedure is repeated several times until a deviation function falls below the preset limit or the preset number of sweeps are executed.

Restrictions on the complexity of the problem

The size of the array XABIN(NB,D), where NB is the number of angular bins and D is the dimension of the representation, can be huge for a large dimensional representation. Since the program works all right with $36 \leq NB \leq 720$, the user may reduce NB to a small number in such cases.

Typical running time

The running time depends on the number of angular bins *Dpts* and the number of sweeps *Rpts*. With *Dpts* = 360 and *Rpts* = 10, the program takes about 10 seconds in the case of He-3 on SUN4m at 100 Mhz. The timings for the parallel version are given in Table 6 of the text.

LONG WRITE-UP

1. Introduction

There are many branches of physics where symmetry breaking is important yet its analysis is highly nontrivial. The Higgs potential and the Coleman–Weinberg potential in the unification theories are difficult to minimize except for simple cases. Extremization of the superpotential in the supersymmetric unification theories is nontrivial. The Landau potential in many branches of condensed matter physics is oftentimes tricky to handle.

The potentials are quartic polynomials of many variables, sometimes hundreds or thousands. Early model builders dealt with only the simplest cases and they could work by hand. However, more complicated models introduced many Higgs particles or a large dimensional order parameter as in He-3. In such cases numerical optimization methods are needed. However, conventional numerical optimization methods are not very useful when the location of the minimum is not unique but degenerate up to the continuous symmetry transformations.

The Michel–Radicati conjecture [1] that a group invariant potential has extrema at a few critical strata corresponding to the maximal little groups was handy and utilized by many model builders [2,3]. The group theoretical method allows one to locate the extrema from the list of maximal little groups without solving the coupled third degree extremum equations. It stirred up considerable research efforts [4–8]. Slansky [2] made lengthy tables of little groups of many representations that could be used in the grand unification model building. Stokes and Hatch [9] made a complete set of tables for the isotropy groups of the irreducible representations of 230 space groups. However, Tolédano [10] found counter-examples to the conjecture. Moreover, the conjecture is less useful for a reducible representation where strata of maximal little groups are oftentimes not one-dimensional critical strata.

A group action transforms a representation vector, which is a representative of an order parameter, onto another equivalent vector. The set of such equivalent vectors is called an orbit. Associated with an orbit is its little group which is a subgroup of the original group and leaves each vector of the orbit unchanged. Two representation vectors along a given direction have identical symmetry properties except that they cannot be transformed onto each other because their lengths are different. A collection of such orbits is called a stratum. The strata of a representation have an interesting geometrical structure which gave rise to the Michel–Radicati conjecture. It will be explained shortly in Section 3.

Some years ago one of the authors [6] devised a geometrical method for finding symmetry breaking directions in the Higgs–Landau problems. The method was practical and could be used for any representation. The key point of the method was the concept of the orbit parameters, which are defined to be the dimensionless ratios

of (*polynomial or non-polynomial*) invariant functions to the unique isotropic quadratic invariant[2]. Thus an orbit parameter is a kind of angular parameter. Such angular parameters were defined earlier in [11] and used in conjunction with a list of little (or isotropy) groups [1,4]. The space of such orbit parameters occupies a confined region, which is called the orbit space. Being defined out of invariants, each point in the orbit space remains unchanged by the symmetry operations and has a definite residual symmetry associated with it, its little group, or sometimes called the isotropy group. Thus a point in the orbit space corresponds to a stratum. Kim showed that the most general quartic Higgs or Landau potential has the absolute minimum at the most protrudent point of the orbit space, which corresponds most likely to one of the critical strata in the case of an irreducible representation but not necessarily so in the case of a reducible representation. He showed that if the Michel–Radicati conjecture is to be valid, the orbit space boundary has to be concave except at the cusps corresponding to the critical strata. Once the orbit space is constructed, then the minimization of the potential and the identification of symmetries are easy. One can easily identify the minimum point, simply by a look at the orbit space when the dimension of the orbit space is two or three.

It has been known [12,13] that the orbit space is a bounded object with a hierarchical structure. The points corresponding to the higher symmetries lie hierarchically closer to the surface of the orbit space and the interior points correspond to the unique lowest symmetry. The points of higher symmetries always form the boundaries of those of lower symmetries. The isolated points corresponding to the highest symmetries are zero-dimensional objects and thus the derivatives of the orbit parameters with respect to the elements of the representation vector, sometimes called the carrier space vector, are zero. Thus, the Michel–Radicati conjecture is a natural consequence of the orbit space structure and thus a group invariant function always has extrema on the critical strata[3] [1,4]. The extrema were also termed as 'inert' phases in the literature [14]. Abud and Sartori [5] elaborated the geometrical structure of the strata of an irreducible representation.

However, there exists not much knowledge about the convexity of the orbit space. We recently showed that the orbit space boundaries of a high-dimensional representation are bound to have many convex boundaries [15]. It was demonstrated with the example of the d-wave superconductor. In such cases a non-maximal little group can be realized. These additional extrema with submaximal little groups which depend on the particular choice of coupling coefficients in the invariant potential were termed as 'non-inert' phases [16,17]. Gufan [4] showed how to find an extremum on non-critical strata.

In order to determine the absolute minimum one has to compare all these extrema. It will be careless to use the Michel–Radicati conjecture blindly. Thus one has to get the full orbit space boundary to be complete. The advantage of Kim's method is that it finds not only the critical strata of maximal little groups but also non-critical strata of submaximal little groups and the phase diagram can be constructed easily. It is powerful if used with the extensive tables made by Slansky [2] and Hatch and Stokes [9]. It is most useful when the representation dimension is large and the orbit space dimension is two or three. Bruder and Vollhardt [17] fully utilized such group theoretical methods for analyzing the Landau potential of He-3 with a 18 component order parameter. Cummins and King [18] used the same method for analyzing the Higgs potential of the 75-dimensional representation of SU(5).

One often deals with the projected subspace of the full orbit space. With respect to the subspace the above hierarchy theorem does not necessarily hold. When the symmetry group is a non-simple group or when the dimension of the representation is large, it is cumbersome to make a list of little groups and the associated invariant directions. When the orbit space boundary is convex, one cannot tell at which level of hierarchy to stop listing. In these cases the above theorem seems to be much less useful.

[2] For a reducible representation the ratio is taken over the product of quadratic invariants of each irreducible representation.

[3] Recently, Michel [13] obtained a criterion for a critical stratum to be a local minimum or maximum in the case of finite groups. He classified all the extrema of invariant functions defined over the Brillouin zones for some arithmetic classes in two and three dimensions.

2. Invariant potentials in spontaneous symmetry breaking

2.1. Landau potential

In order to phenomenologically explain the symmetry changes occurring during a phase transition in condensed matters, Landau devised the concept of the multi-component order parameter, η_a, $a = 1, \ldots, M$. The order parameter transforms according to a particular representation (n) of the symmetry group G of the physical system at high temperature,

$$\eta'_a = \sum_b R^{(n)}_{ab}(g)\eta_b\,, \tag{1}$$

where g is an arbitrary element of G and $R^{(n)}(g)$ is a matrix representing g according to the representation (n). The thermodynamic potential of a symmetric physical system remains invariant under these symmetry transformations. If it is expanded in power series, it should be of the form [4,11]

$$V(T, P; \eta) = \tfrac{1}{2}A\sum_a \eta_a^2 + \tfrac{1}{3}\sum_i C_i\theta_i^{(3)}(\eta_a) + \tfrac{1}{4}\sum_i B_i\theta_i^{(4)}(\eta_a)\,, \tag{2}$$

where the coupling coefficients A, C_i and B_i are functions of temperature T and pressure P and $\theta_i^{(3)}(\eta_a)$ and $\theta_i^{(4)}(\eta_a)$ are independent invariant polynomials of degree three and four, respectively.

At temperatures higher than the critical temperature, the coefficient A of the quadratic term is positive and the minimum of the potential V is located at $\eta = 0$. This means that the stable state of the system is a symmetric state and does not prefer any direction in the η-space. When the temperature is lowered below T_c, A becomes negative and the minimum of the potential occurs at a nonzero η_0. The stable state of the system is no longer symmetric under all the symmetry elements of G and prefers a particular direction. However, the system is still symmetric under those symmetry elements h_α of G that leave η_0 unchanged. These h_α form a subgroup H of G, called a *little group* of η_0.

Starting with a symmetric potential, Landau could explain the occurrence of a smaller symmetry as a subgroup of the high temperature symmetry group. It is the state of the potential minimum that determines the ultimate symmetry of the system. This mechanism is termed *spontaneous symmetry breaking*. Landau's phenomenological theory of phase transition is useful for symmetry classification and thus widely used in condensed matter physics. Many reviews and books on this subject have been published (see [19]).

2.2. Higgs potential

In the early 1970's the longstanding problem of generating gauge boson masses without destroying the renormalizability was solved by the introduction of the scalar particles. The Lagrangian is built as a symmetric function of gauge bosons, fermions, and scalar particles. The scalar potential is also of the form (4). By adjusting the coupling coefficients, the minimum of the Lagrangian can be made to occur along a particular direction of the scalar fields so that a preferred symmetry can be preserved. Since the formal symmetry of the Lagrangian is the same before and after symmetry breaking, the renormalizabilty of the Lagrangian remains intact. The unification of the weak and electromagnetic interactions was possible due to employment of spontaneous symmetry breaking.

Ever since the success of electroweak unification, a flurry of research activities arose in grand unification theories and SUSY grand unification theories. Though there have been attempts to search the dynamical symmetry breaking mechanism, the method of spontaneous symmetry breaking with a complex family of scalar particles was widely used. As sophisticated unification models require high-dimensional representations of scalar fields, the task of locating the minimum of the scalar potential has become highly nontrivial. Except for simple

Table 1
The little groups and orbits of the adjoint representation of SU(5)

level	little group	η
1	$SU(3)\times SU(2)\times U(1)$	$[a,a,a,-\frac{3}{2}a,-\frac{3}{2}a]$
1	$SU(4)\times U(1)$	$[a,a,a,a,-4a]$
2	$SU(3)\times U(1)\times U(1)$	$[a,a,a,b,-3a-b]$
2	$SU(2)\times SU(2)\times U(1)\times U(1)$	$[a,a,b,b,-2a-2b]$
3	$SU(2)\times U(1)\times U(1)\times U(1)$	$[a,a,b,c,-2a-b-c]$
4	$U(1)\times U(1)\times U(1)\times U(1)$	$[a,b,c,d,-a-b-c-d]$

cases it requires numerical methods. Since the entire continuous set of orbits of a particular representation vector which minimizes the potential yield the same potential value, conventional numerical methods can run into trouble. Furthermore, due to the continuous gauge symmetry some components of the scalar field can be gauged away. It is not easy to find which components can be eliminated. In the Landau theory a single irreducible representation of order parameter is used usually, whereas many irreducible representations of scalars are employed in unification theories. Thus the Higgs problem is much richer than the Landau problem. A comprehensive review on this subject can be found in [20].

3. Orbits, little groups, integrity basis, and orbit space

3.1. Orbits and little groups

An *orbit* of a particular representation vector η_0 is the set of vectors obtained by acting all the symmetry elements of the group G,

$$\eta_0^G \equiv \{\eta_0' = M(g)\cdot\eta_0, \text{ for all } g\in G\}. \tag{3}$$

A particular vector η_0 is invariant under the actions of the symmetry elements belonging to its little group, $H_0 \subset G$. Another vector η_0' on the orbit of η_0 preserves its own little group H_0', which is equivalent to H_0: $H_0' = g^{-1}H_0 g$.

All possible little groups of a representation vector are subgroups of G and they have hierarchical relationships among each other. Slansky [2] published a table of little groups for scalar representations of those groups frequently used in unification theories. A concrete example of such hierarchy can be found in [18]. Stokes and Hatch [9] published a table of isotropy subgroups of all the space group representations associated with special points on the Brioullin zone boundaries. Simple examples can be found in [21].

The space of representation vectors also has the same hierarchical structure as their little groups. Thus the geometry of the orbit space is deep-rooted in the group theoretical nature of the representation. Let us illustrate this relation with the 24-dimensional adjoint representation of SU(5). With a SU(5) gauge transformation η can be reduced to a traceless diagonal 5×5 matrix. It has two level-1 little groups, two level-2 little groups, one level-3 little group and the unique highest level little group as tabulated in Table 1. We note that $SU(3)\times SU(2)\times U(1)$ is a supergroup of $SU(3)\times U(1)\times U(1)$ and $SU(2)\times SU(2)\times U(1)\times U(1)$ and so is $SU(4)\times U(1)$. The orbit $[a,a,a,-\frac{3}{2}a,-\frac{3}{2}a]$ is a special case of $[a,a,a,b,-3a-b]$ and $[a,a,b,b,-2a-2b]$ and so is the orbit $[a,a,a,a,-4a]$.

We notice that the orbits of level-l little groups have l free parameters. There must be some conditions among the components of the representation vector. There is another way to represent orbits than listing their components, which we will see in the next subsection.

3.2. Integrity basis and orbit space

There exists a set of basic invariant homogeneous polynomials for a given representation [22,23]. The set is called the *integrity basis*. In fact, there are two kinds of basic invariant polynomials, the denominator invariants θ_i and the numerator invariants φ_j. Then an arbitrary invariant polynomial can be written as a polynomial of these basic invariants as follows:

$$V(\eta) = P(\theta_i) + \sum_{j=1}^{N} Q_j(\theta_i)\varphi_j\,, \tag{4}$$

where P and Q are polynomials in θ_i. The denominator invariants are algebraically independent invariant polynomials. But products of the numerator invariants can be written in a form (4) and thus they are not algebraically independent. If the symmetry group G is a finite group, the number M of denominator invariants θ_i is equal to the dimension of the representation vector. For a continuous group, a gauge transformation reduces M by the number of generators of G minus the number of generators of the smallest little group of the generic orbit. Though there is a way to compute the numbers and degrees of denominator and numerator invariants, it is a little complicated and we refer the interested reader to [23].

The Landau potential and the Higgs potential are of the form (4). Due to the requirement of renormalizability the Higgs potential is expanded only up to the fourth degree. The Landau potential is expanded up to the fourth degree if one considers a continuous phase transition only. Thus the invariant potentials are not expanded to full extent and only a subset of the integrity basis is used.

Since an invariant function of a representation vector has the same value on an orbit of a particular representation vector, it can be used to specify an orbit. An *orbit parameter* is defined to be a ratio of a basic invariant to the $(d_i/2)$th power of the unique quadratic invariant $\theta_0 = \sum_a \eta_a^2$ (d_i is the degree of θ_i),

$$\vartheta_i = \theta_i/\theta_0^{d_i/2}\,. \tag{5}$$

Then an orbit is completely specified by θ_0 and $(M-1)$ orbit parameters ϑ_i that contain directional information.

The *orbit space* $(\vartheta_1, \vartheta_2, \ldots, \vartheta_{(M-1)})$ exhibits the hierarchical nature. There are cusps joined by curves, which form the boundaries of two-dimensional surfaces, etc. The innermost points correspond to the unique generic orbit with the smallest symmetry. A few examples will be shown later in the paper. We refer the reader to [24] for ample examples. Since the hierarchical structure stems from the group theoretical nature of the representation, the 'orbit space' defined through non-polynomial invariant functions such as the logarithmic function appearing in the Coleman–Weinberg potential also exhibits the hierarchical structure to some extent [25,26].

The level-1 orbits are zero-dimensional points in the orbit space and thus satisfy a set of conditions

$$\frac{\partial \vartheta_i}{\partial \eta_a} = 0 \quad \text{for all } i, a\,. \tag{6}$$

The level-2 orbits are one-dimensional curves and satisfy the conditions

$$\frac{\partial \vartheta_i}{\partial \eta_a}\frac{\partial \vartheta_j}{\partial \eta_b} = \frac{\partial \vartheta_j}{\partial \eta_a}\frac{\partial \vartheta_i}{\partial \eta_b} \quad \text{for all } i, j, a, b\,. \tag{7}$$

The condition (6) is very useful for locating a potential minimum. One may consider a potential as a function of $r^2 \equiv \theta_0$ and the orbit parameters ϑ_i as well as the representation vector η. Then in order to locate a minimum, one would try to solve

$$\frac{\partial V}{\partial r} = 0\,, \tag{8}$$

$$\sum_i \frac{\partial V}{\partial \vartheta_i}\frac{\partial \vartheta_i}{\partial \eta_a} = 0. \tag{9}$$

But Eq. (9) is already satisfied on the level-1 orbits, called *critical orbits*. Critical orbits are also called 'inert' phases because they satisfy the extremum conditions regardless of coupling coefficients A, B_i and C_i. It seems that one only needs to solve Eq. (8) [1,4].

This is what Michel and Radicati [1] called the maximality conjecture. The conjecture has been widely used among Landau theorists and unification model builders. Kim [6] clarified the condition that the maximality conjecture hold. The orbit space boundary must be concave except at cusps. Otherwise the minimum may occur on the curves or surfaces corresponding to non-maximal little groups. In such cases one can still take advantage of Eq. (7) and locate the minimum on a higher level orbit as explained by Gufan [4]. Kim's method will be described in more detail in Section 5.1. Although the hierarchical nature and the singularity conditions were known among mathematicians, nothing is known about the concavity of the orbit space.

Several counter examples have been found in [10,27,28]. In [28] a cusp with non-maximal little group was found and in other cases [10,27] minima were found on the curves. It was shown [15] that the orbit space of high-dimensional representation is bound to have convex boundary curves due to lack of sufficient number of maximal little groups. We are planning to address this issue in future.

After Kim demonstrated the advantage of using the orbit space, his method was employed in several problems [17,18]. It requires a careful group theoretical analysis of little group chains of a given representation. One needs to construct a list like Table 1. However, it is much less painful than the conventional method of solving Eqs. (8) and (9) in the η-space directly. For space group representations the complete lists are tabulated in [9]. As Cummins and King [18] noted, one cannot be sure that one has found the full orbit space boundary until one exhausts all the levels, which is prohibitively laborious for a high-dimensional representation of a continuous group. Furthermore, critical orbits corresponding to non-maximal and discrete subgroups cannot be found from the usual hierarchical list.

4. Algorithm for Monte Carlo search of the orbit space

It is necessary to have an alternative method for building the orbit space. Simple Monte Carlo methods that were tried in the past [5,6] were not efficient for obtaining the orbit space boundary. We have devised a more efficient Monte Carlo method for building the orbit space. It is applicable to any representation and robust. The algorithm uses the von Neumann rejection method [29] and the over-relaxation method.

Suppose that we are searching for the boundary curves of a two-dimensional orbit space, (θ, ϕ). Let us assume that the orbit parameters θ and ϕ are functions of M variables, x_m. Then our algorithm is stated as follows:

(1) Initially *Ipts* points are sampled in a uniformly random way. That is, *Ipts* sets of x_m are sampled in a uniformly random way from the interval $[-1, 1]$. Then one computes the center of gravity, (θ_C, ϕ_C), of these *Ipts* points, (θ_i, ϕ_i).

(2) For the *Ipts* points, one computes the angle of the vector, $(\theta_i - \theta_C, \phi_i - \phi_C)$ and assigns an angular bin. Let the total number of bins be *Dpts*.

(3) One then identifies the outermost points along each of the *Dpts* discrete directions. The 'outwardness' is defined to be the distance of the point from the center of gravity.

(4) Starting from each of these selected points, a random walker with M-legs makes moves by moving one of its legs, x_m. If the move increases the distance, it is accepted. If not, the random walker steps the leg in the opposite direction with a different stride. If the move increases the distance, it is accepted. Otherwise it is rejected and the old value of x_m is retained.

If the random walker jumps over into another angular bin, its position is compared with the current outermost point along that direction. The more distant of the two is selected as the new outermost point in that angular bin.

(5) Step 4 is repeated for all x_m.
(6) Steps 4 and 5 are repeated along all the angular directions.
(7) Steps 4, 5 and 6 are repeated a finite times *Rpts* or until no further appreciable improvements are made within the allowed number of trials.
(8) The search of the orbit space boundary is completed.

The circumference of the orbit space is discretized into *Dpts* bins and the outermost point in each bin is sought after. In the random search for the boundary points the random walker of a selected bin is encouraged when it moves towards the surface. If a move $x_m \to x_m + \delta$ is unsuccessful then another move $x_m \to x_m - \omega \cdot \delta$ is tried, where ω is an adjustable relaxation parameter. Even when the random walker strays into another direction, its move is not discarded but compared with the current outermost point. In this way the random walker finds the outward direction in a few attempts. Therefore the convergence rate is fast.

5. Applications

5.1. d-wave superconductor

Recently there have been some activities to search for anisotropic superconductivity [3]. It has been confirmed that a d-wave pairing actually occurs [30]. We have been investigating a model of an abnormal superconductor with the high temperature symmetry [15] $G \equiv \mathrm{O}(3)\times\mathrm{U}(1)\times\mathrm{T}$. For the spin-0 d-wave gap functions the 3-dimensional symmetric traceless complex representation, Φ_{ij}, is assumed for the order parameter. Under O(3) the indices i, j transform like a three-dimensional vector. The U(1) transforms $\Phi \to e^{i\lambda}\Phi$ and $\Phi^* \to e^{-i\lambda}\Phi$. The time reversal symmetry T transforms $\Phi \to \Phi^*$ and vice versa.

Then the most general Landau potential up to the fourth degree in Φ can be written as a polynomial of the basic invariant polynomials,

$$V(\Phi) = \alpha I_0 + \gamma_0 I_0^2 + \gamma_1 T_1 + \gamma_2 T_2 . \tag{10}$$

Each basic invariant polynomial is defined as follows:

$$I_0 = \mathrm{Tr}(\Phi\Phi^*) , \tag{11}$$

$$T_1 = \mathrm{Tr}(\Phi\Phi^*\Phi\Phi^*), \quad T_2 = \mathrm{Tr}(\Phi\Phi\Phi^*\Phi^*) . \tag{12}$$

It is obvious that these are invariant under the symmetry group G.

The orbit parameters θ and ϕ are defined as

$$\theta \equiv \frac{T_1}{I_0^2} , \quad \phi \equiv \frac{T_2}{I_0^2} . \tag{13}$$

Along the chosen direction (θ, ϕ), the Landau potential has a directional minimum value [6],

$$V_0(\theta, \phi) = -\frac{1}{4}\frac{\alpha^2}{(\gamma_0 + \gamma_1\theta + \gamma_2\phi)} , \tag{14}$$

and the absolute minimum occurs along a direction where $(\gamma_0 + \gamma_1\theta + \gamma_2\phi)$ has the smallest value. The contour of directional minima are lines and the absolute minimum is located at the most protrudent boundary point. If there is a convex boundary curve more protrudent than the cusps then the absolute minimum occurs at a point where a line makes a tangential contact with the convex boundary.

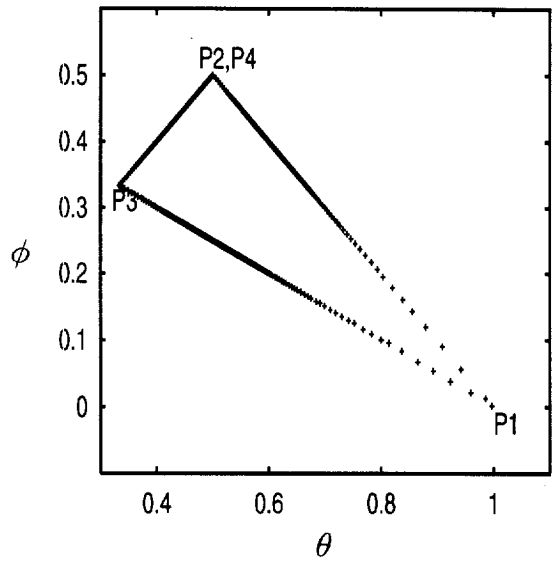

Fig. 1. The orbit space (θ, ϕ) of d-wave superconductor.

By choosing an appropriate basis, we can always have one of the two real matrices in a diagonal form. So there are actually 7 independent components in Φ_{kl}. We can define these 7 independent components like

$$\Phi_{ij} \equiv \begin{pmatrix} a & 0 & 0 \\ 0 & b & 0 \\ 0 & 0 & -a-b \end{pmatrix} + i \begin{pmatrix} s & u & v \\ u & t & w \\ v & w & -s-t \end{pmatrix}. \tag{15}$$

The orbit space, (θ, ϕ), is a triangle with vertices at P1=(1.0,0.0), P2=(0.5,0.5), and P3=$(0.\dot{3},0.\dot{3})$ as shown in Fig. 1. P1 is associated with the set of variables, $(a = 1, b = -1, s = t = 0, u = 1, v = w = 0)$, and its little group is $D_{4h} \times e^{i\pi} \times T$. P2 is overlapped by two cusps, $p_2 = (a = 1, b = 1, s = t = u = v = w = 0)$ corresponding to $O^z(2) \times T$ and $p_4 = (a = 1, b = -1, s = t = u = v = w = 0)$ corresponding to $D_{4h} \times e^{i\pi} \times T$. P3 is associated with $(a = 1, b = Q, s = Q, t = 1, u = v = w = 0)$ with $Q = -2 - \sqrt{3}$ and corresponds to the little group $D_{4h} \times e^{i\pi/2} \times T$. For more details we refer the reader to [15].

The Landau potential (10) truncated at the fourth degree can have no lower symmetry than those of these four points. The degeneracy at P2 can be lifted if we include the sixth degree terms.

5.2. Helium-3

For the p-wave pairing model of superfluid Helium-3, a 3×3 complex matrix, Φ_{ij}, is assumed for the order parameter [14,16,17]. Under $G = SO(3)_S \times SO(3)_L \times U(1)$, the index i transforms like a three-dimensional vector in the spin space and j like in the coordinate space.

Then the most general Landau potential for the free-energy difference between the normal and superfluid phases, up to the fourth degree in Φ, can be written as a polynomial of the basic invariant polynomials,

$$V(\Phi) = \alpha I_0 + \gamma_0 I_0^2 + \gamma_1 S_1 + \gamma_2 S_2 + \gamma_3 S_3 + \gamma_4 S_4 . \tag{16}$$

Each basic invariant polynomial is defined as follows:

$$I_0 = \mathrm{Tr}(\Phi\Phi^\dagger) , \tag{17}$$

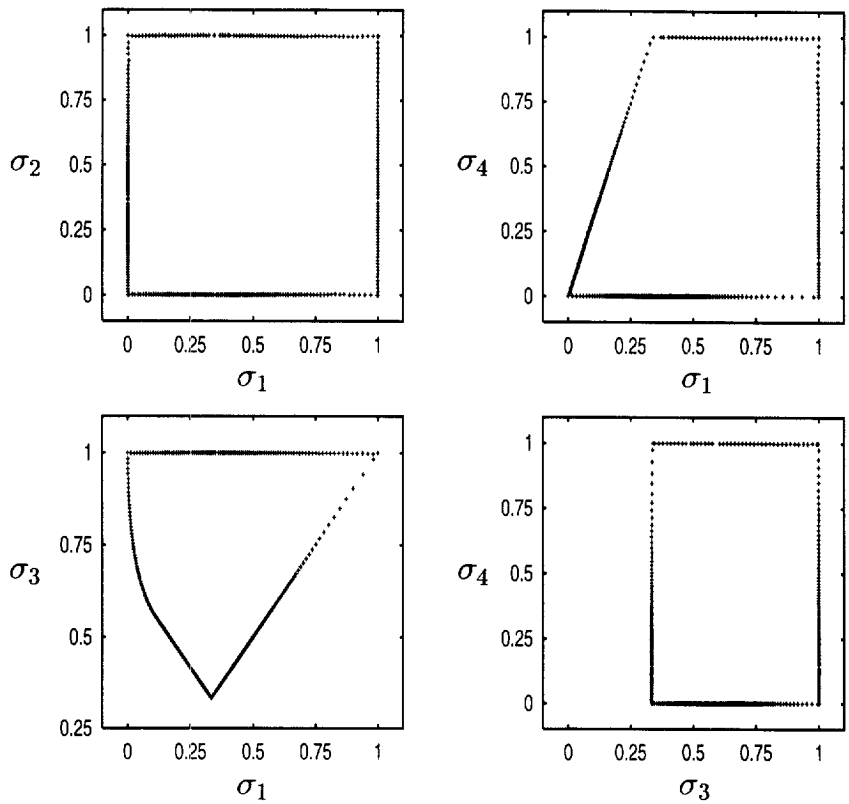

Fig. 2. The orbit spaces: (σ_i, σ_j) of He-3. (σ_1, σ_3) and (σ_2, σ_3) are identical and (σ_1, σ_4) and (σ_2, σ_4) are identical.

$$S_1 = \mathrm{Tr}[(\Phi^\dagger\Phi)(\Phi^\dagger\Phi)^*], \qquad S_2 = \mathrm{Tr}[(\Phi\Phi^\dagger)(\Phi\Phi^\dagger)^*],$$
$$S_3 = \mathrm{Tr}[(\Phi\Phi^\dagger)(\Phi\Phi^\dagger)], \qquad S_4 = |\mathrm{Tr}(\Phi\Phi^T)|^2. \tag{18}$$

Now we have a four-dimensional orbit space. Our algorithm is applicable to a high-dimensional orbit space without major revision. However, in this paper let us limit ourselves to two-dimensional subspaces. Let us define the orbit parameters σ_i as

$$\sigma_1 \equiv \frac{S_1}{I_0^2}, \qquad \sigma_2 \equiv \frac{S_2}{I_0^2}, \qquad \sigma_3 \equiv \frac{S_3}{I_0^2}, \qquad \sigma_4 \equiv \frac{S_4}{I_0^2}. \tag{19}$$

The orbit spaces, (σ_i, σ_j), are shown in Fig. 2. There are eight cusps of critical strata. These were referred to 'inert phases' in [14]. Their locations are listed in Table 2. The orbit spaces in Figs. 2a, 2c and 2d are all polygons. The boundary portion joining P3 and P6 in Fig. 2b is a convex curve corresponding to non-maximal little groups whereas the other portions are straight lines. Thus non-maximal symmetries can be realized in a certain region of the parameter space (γ_i) [14,16,17]. We notice that the two phases P2 and P5 cannot be realized because they are not protrudent on the boundary. This was clarified in [16].

5.3. SU(5) unification theory

In the SU(5) unification theory [31] the gauge symmetry may be broken down to $\mathrm{SU}(3)\times\mathrm{SU}(2)\times\mathrm{U}(1)$ by a Higgs multiplet Φ transforming like an adjoint representation. Φ is a 5×5 Hermitian traceless matrix which

Table 2
The critical strata (inert phases) of maximal little groups, orbit representatives, orbit parameters; $\omega \equiv \exp(-2\pi i/3)$

Label	Φ	$(\sigma_1, \sigma_2, \sigma_3, \sigma_4)$	Nomenclature
P1	(1,0,0),(0,0,0),(0,0,0)	(1,1,1,1)	polar
P2	(1,0,0),(0,1,0),(0,0,0)	(0.5,0.5,0.5,1)	planar
P3	(1,0,0),(0,1,0),(0,0,1)	$(0.\dot{3},0.\dot{3},0.\dot{3},1)$	isotropic, BW
P4	$(1,0,0),(0,\omega,0),(0,0,\omega^2)$	$(0.\dot{3},0.\dot{3},0.\dot{3},0)$	α
P5	(1,0,0),(0,i,0),(0,0,0)	(0.5,0.5,0.5,0)	bipolar
P6	(1,i,0),(0,0,0),(0,0,0)	(0,1,1,0)	axial, ABM
P7	(1,0,0),(i,0,0),(0,0,0)	(1,0,1,0)	β
P8	(1,i,0),(i,−1,0),(0,0,0)	(0,0,1,0)	A_1

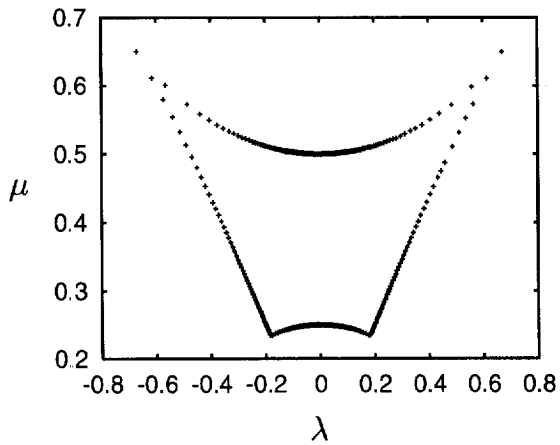

Fig. 3. The orbit space of SU(5) adjoint.

can be diagonalized by a unitary transformation. Thus we have $\Phi = \mathrm{diag}[a, b, c, d, -a-b-c-d]$. The basic invariants are

$$I_0 = \mathrm{Tr}\,\Phi^2, \qquad I_3 = \mathrm{Tr}\,\Phi^3, \qquad I_4 = \mathrm{Tr}\,\Phi^4, \qquad I_5 = \mathrm{Tr}\,\Phi^5. \tag{20}$$

Let us again limit ourselves to the two-dimensional subspace, ($\lambda \equiv I_3/I_0^{(3/2)}$, $\mu \equiv I_4/I_0^2$). Its shield shaped orbit space (Fig. 3) was obtained using the group theoretical method in [24]. There are four cusps, $\mathrm{P1}_\pm = (\pm 3/\sqrt{20}, 13/20)$ and $\mathrm{P2}_\pm = (\pm 1/\sqrt{30}, 7/30)$. They correspond to $\Phi(\mathrm{P1}_+) = \mathrm{diag}[a, a, a, a, -4a]$, $\Phi(\mathrm{P1}_-) = -\Phi(\mathrm{P1}_+)$, $\Phi(\mathrm{P2}_+) = \mathrm{diag}[2a, 2a, 2a, -3a, -3a]$, and $\Phi(\mathrm{P2}_-) = -\Phi(\mathrm{P2}_+)$. The little group of $\mathrm{P1}_\pm$ is SU(4)×U(1) and that of $\mathrm{P2}_\pm$ is SU(3)×SU (2)×U(1).

Using the parallel version of our program, we have computed the orbit space of the 75-dimensional representation of SU(5) and obtained a similar result as obtained by Cummins and King [18]. It will be published separately in future.

6. Variables and subroutines of the program

There are two programs, the sequential version He_3.f and the parallel version He_3par.f. The sequential program follows the steps explained in Section 4. The parallel program follows the steps explained in Section 8. We list variables and subroutines with brief descriptions. The lines marked with * refer to the parallel version.

```
  Variables.
       D:      dimension of order parameter
       XA:     array for order parameter components
               passed to COMORB, UPDATE and NEW_RW thru common block FARG
       XABIN:  array for order parameter yielding DMAX
               passed to UPDATE and NEW_RW thru common block XARR
       DMAX:   array for random walker's position
               passed to UPDATE and NEW_RW thru common block XARR
       DPTS:   number of angular bins
       RPTS:   number of Monte Carlo sweeps
       ERRO:   bound for area increment
       DEL:    delta
       DRX:    omega
       SUCC:   success rate
       DEVI:   area increment between MC sweeps
*      MYNUM:  node number
*      NPROC:  number of nodes

  Subroutines
       UPDATE:  random walker marches towards the boundary
       RW_MOVE: traces random walker's move
       NEW_RW:  appoints a new random walker
       DEVIATN: computes area increment
       ANGLE:   computes the polar angle of (X,Y)
       COMORB:  computes the orbit parameters
*      EXCHANGE: exchanges DMAX globally, updates it locally and then
*                globalize it again

  Paragon specific routines
*      CSEND:    sends messages to other node
*      CRECV:    receives messages from other node
*      CSENDRECV: sends and receives messages
*      GSSUM:    sums globally (float)
*      GISUM:    sums globally (integer)
*      GCOLX:    concatenates data globally
*      DCLOCK:   timing routine
```

7. Performance tests

7.1. Success rate

The success rate was computed in the following way. A random walker of an angular bin b makes a move,

$$x_i^{(k+1)} = x_i^{(k)} + \delta \cdot v\,, \tag{21}$$

where δ is the stride and v is a random number in the interval $[-1, 1]$. The routine `Angle` computes the angular bin number a of the new position, (θ, ϕ), and the routine `Distance` computes its distance d from the center of gravity, (X_c, Y_c). The original bin number b and the new one a need not be the same. Actually, a considerable

Table 3
Success rates of 100-run MC experiments. Each run consists of 20 MC sweeps. The success rate of each run is measured and then averaged over 100 runs.

δ	A	B	C
0.1	0.3762	0.3792	0.4440
0.2	0.3350	0.3228	0.4403
0.3	0.3115	0.3014	0.4406
0.4	0.2976	0.2915	0.4406
0.5	0.2896	0.2860	0.4401

portion $\sim 5\%$ of times b is not the same as a. They can be tens of angular bins away when $Dpts = 360$. Since we are looking only $Dpts$ directions these strayers are not disposable. The array DMAX contains the maximum distance along each angular bin. If DMAX[a] is smaller than d then DMAX[a] is replaced with the new value d and $x_i^{(k+1)}$ is saved in a two-dimensional array XMAX[i,a] for use in the next MC sweep. If DMAX[a] is not smaller than d then another move in the opposite direction is made,

$$x_i^{(k+1)} = x_i^{(k)} - \omega \cdot \delta \cdot v\,, \tag{22}$$

where ω is the relaxation parameter. The angular bin number a' and the distance d' are computed. DMAX[a'] is checked against d' and the necessary bookkeeping is done. If the second move fails then it is considered a failure and the count FAIL is incremented. The variable x_i retains the old value in this case. Every time the routine Comorb which computes θ and ϕ is called, the count ICC is incremented. One Monte Carlo sweep is executed when random walkers in all $Dpts$ angular bins are updated once. One Monte Carlo run consists of $Rpts$ sweeps. The success rate of a Monte Carlo run is computed as

$$\text{SUCCESS} = 1 - (\text{FAIL}/\text{ICC})\,. \tag{23}$$

We measured the average of the success rates in a 100 run experiment with different sets of (δ, ω). We list the results in Table 3 where ω is fixed at 0.35. As δ is increased the success rate decreases in the cases of A (Section 5.1) and B (Section 5.2). It is noteworthy that the success rates in the two cases of similar invariant functions are about the same regardless of the dimension M. In case C (Section 5.3) it stays constant at $\sim$0.44. Our algorithm does not remember the direction of a random move. If we use an array for δ to differentiate the angular bins and adjust the signs and magnitudes of $\delta[i]$, the success rate will be improved. Nonetheless, our simple algorithm seems to be reasonably efficient.

7.2. Accuracy and convergence

In order to measure the accuracy of the algorithm we need to define a performance criterion. One good criterion is to measure the distances of random walkers from the orbit space boundaries. We define the deviation function $\Delta(\alpha)$ in a particular Monte Carlo run as follows:

$$\Delta(\alpha) = \sum_{i=1}^{Dpts} \sqrt{(x_i - x_b(x_i, y_i))^2 + (y_i - y_b(x_i, y_i))^2}/Dpts\,, \tag{24}$$

where $[x_b(x_i, y_i), y_b(x_i, y_i)]$ are coordinates of the point where a line passing through the random walker at (x_i, y_i) meets the nearest boundary line perpendicularly. Since the orbit space of case A in consideration is known to be a triangle it is easy to compute the deviation function. For an orbit space with known curved boundaries like case C, the deviation function may be defined similarly but it will be more difficult to compute.

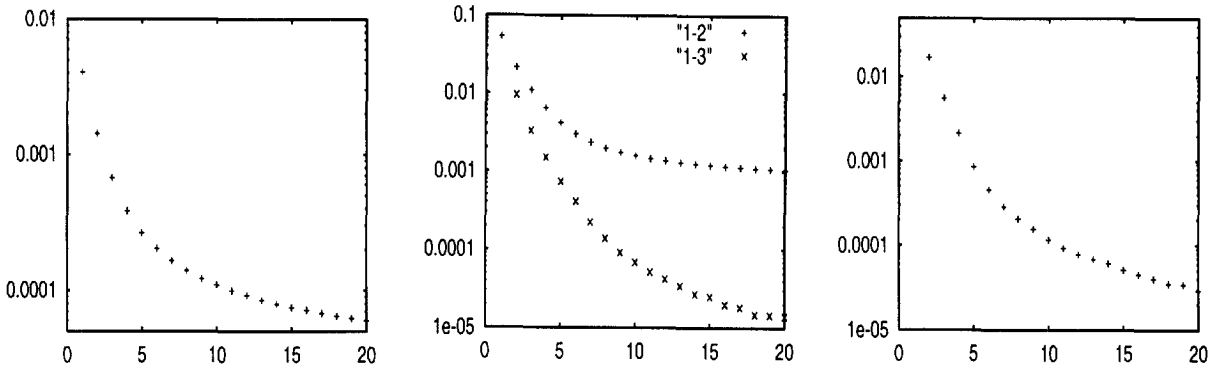

Fig. 4. The deviation functions: $\bar{\Delta}(r)$. The abscissa is the MC sweep count r and the ordinate is $\bar{\Delta}$. The left one is for case A with Eq. (24). The middle one is for case B: the upper curve is for (σ_1, σ_2) with Eq. (24) and the lower curve is for (σ_1, σ_3) with Eq. (26). The right one is for case C with Eq. (26).

In general we do not know a priori the orbit space boundaries and thus we need a more practical definition. An area function can be defined to be

$$\mathcal{A}(\alpha) = \sum_{i=1}^{Dpts} \sqrt{(x_i - X_c(\alpha))^2 + (y_i - Y_c(\alpha))^2}/Dpts\,, \tag{25}$$

where (X_c, Y_c) are the coordinates of the center of gravity which depend on a particular choice of initial points. $\mathcal{A}$ is proportional to the two-dimensional area of the orbit space. As random walkers move outwards it is maximized and the program may be stopped when no further appreciable improvements are made. If we use the center of gravity obtained from initial points this definition is useful only within a particular run. $\mathcal{A}$'s of independent runs cannot be compared. However, if we *fix* the center of gravity regardless of initial points then $\mathcal{A}$'s of independent runs have the same meaning and may be averaged.

Since we do not know the exact value of $\mathcal{A}$ a priori, we can only measure the difference between successive sweeps and we define the deviation function, less rigorous but useful in general,

$$\Delta[\alpha; r] \equiv (\mathcal{A}[\alpha; r] - \mathcal{A}[\alpha; r-1])\,. \tag{26}$$

After each sweep r over all angular bins we measure $\Delta[\alpha; r]$ and store it in an array `DEV[r]`. Then we take ensemble averages of these deviation functions. Thus we measure

$$\bar{\Delta}[r] = \sum_{\alpha=1}^{N} \mathtt{DEV[r]}/N\,. \tag{27}$$

The results of a 100 MC run experiment for all cases with $\delta = 0.1$ and $\omega = 0.35$ are shown in Fig. 4. Fig. 4a is for case A, 4b for B and 4c for C. In Fig. 4b, the data marked "1-2" $(\sigma_1 - \sigma_2)$ was obtained using the deviation function (24) and the data marked "1-3" $(\sigma_1 - \sigma_3)$ was obtained with Eq. (26). We see that they exhibit the familiar relaxation behavior of a variance in a Monte Carlo simulation.

We repeated this experiment with different sets of (δ, ω). The results are illustrated in Fig. 5. In case A we found that the set $(\delta = 0.15, \omega = 0.45)$ is the optimum choice, namely that it yields the lowest curve in the Fig. 5a. The optimum set for case B was $(\delta = 0.60, \omega = 0.30)$ and for the SU(5) adjoint it was $(\delta = 0.10, \omega = 0.25)$. Notice that the optimum sets for the maximum success rate and the minimum deviation are not the same.

However, the magnitudes of the deviation functions depend on the dimension of the order parameters. We give the numerical results of a 100 MC run experiment obtained along with Fig. 1 and Fig. 2a in Table 4.

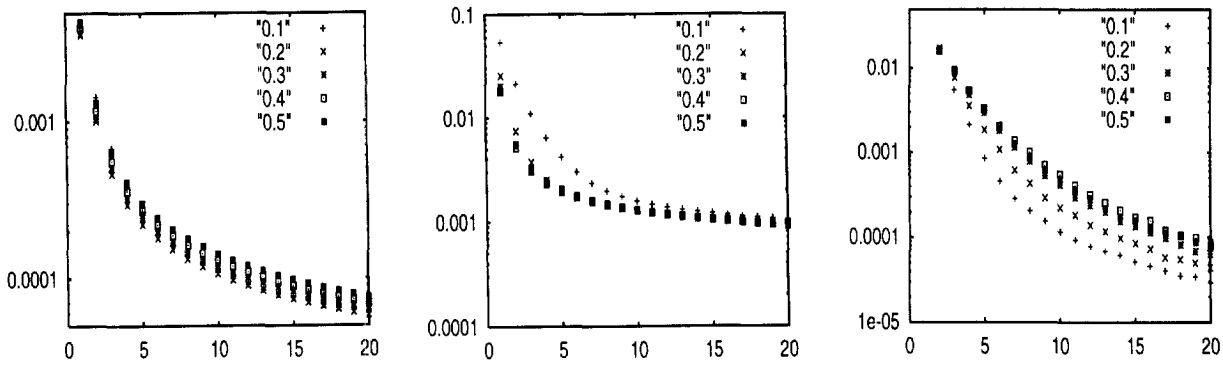

Fig. 5. The deviation function at different values of δ: $\bar{\Delta}(r, \delta)$. The abscissa is the MC sweep count r and the ordinate is $\bar{\Delta}$. The numbers marking the symbols are the values of δ. From left to right they are for cases A, B and C. ω is set at 0.35.

Table 4
The deviation function (24) measured in a 100 run MC experiment, with ($\delta = 0.1, \omega = 0.35$) as depicted in Fig. 4

r	$M = 7$	$M = 18$
1	0.4058E−02	0.5341E−01
2	0.1426E−02	0.2114E−01
3	0.6721E−03	0.1085E−01
4	0.3819E−03	0.6405E−02
5	0.2636E−03	0.4174E−02
6	0.2025E−03	0.2990E−02
7	0.1655E−03	0.2337E−02
8	0.1403E−03	0.1963E−02
9	0.1219E−03	0.1735E−02
10	0.1095E−03	0.1573E−02
11	0.9920E−04	0.1457E−02
12	0.9139E−04	0.1372E−02
13	0.8431E−04	0.1304E−02
14	0.7919E−04	0.1250E−02
15	0.7478E−04	0.1204E−02

In both cases we used the same definition of the deviation function (24). In case A ($M = 7$) a deviation of magnitude $\sim 0.15 \times 10^{-2}$ is obtained with $r \approx 2$ whereas in case B ($M = 18$) it takes about ten sweeps ($r \approx 10$) to get the same accuracy. Thus the required number of sweeps to get a given accuracy increases with the dimension M. However, the deviation functions seem to reach plateaus. Once it reaches a plateau, more MC sweeps do not improve the accuracy appreciably and the program must be stopped.

7.3. *Initial sampling*

We also tried how many initial samplings *Ipts* are sufficient. It was not as critical as other parameters. *Ipts* ≈ 2000 was enough in all cases. This means that the dimension M is irrelevant in choosing *Ipts*. What is relevant is the number of angular bins *Dpts*. 5∼6 initial samplings per bin seems to be enough. If there are many singular curves and surfaces on the full orbit space boundary the random walker easily gets trapped at these singularities. One way to avoid this situation is to run many Monte Carlo runs with different initial points.

Table 5
A mapping of arrays representing random walkers onto the 4 processing elements

PE	DMAX	XMAX
0	[1:90]	[*,1:90]
1	[91:180]	[*,91:180]
2	[181:270]	[*,181:270]
3	[271:360]	[*,271:360]

8. Parallel implementation

8.1. Domain decomposition

The number of Higgs particles in unification theories are huge reaching thousands in some models. Theorists relied on the Michel–Radicati conjecture. As we explained in [15], the orbit space boundaries are normally convex when the dimension M is large. Thus non-maximal little groups are realized and the conjecture is only partially useful. In this case the required amount of computation is enormous and may take months or years on a modern workstation. Massively parallel supercomputers provide practical means for this kind of programs.

Since the random walkers are independent, most of the time the angular bins may be distributed among many processor elements, PEs. However, when a random walker belonging to PE A strays into a bin belonging to another PE B this information needs to be sent to PE B. This communication need not be carried out immediately. One can wait until each PE finishes a sweep through its own angular bins.

After each sweep the arrays DMAX and XMAX must be updated. To be concrete, let us assume $Dpts = 360$ and the number of PEs $N_p = 4$. Then the mapping between PEs and the array elements may be given as in Table 5.

8.2. Communication

After each sweep a communication routine Exchange is called. It assumes a ring shape connection topology. The routine sends and receives the arrays by calling a system routine Sendrecv $(N_p - 1)$ times. Initially each PE prepares a send buffer CBUF in the following way. PE 0 copies DMAX[91:360] to CBUF[1:270]. PE 1 copies DMAX[181:360] to CBUF[1:180] and DMAX[1:90] to CBUF[181:270]. PE 2 copies DMAX[271:360] to CBUF[1:90] and DMAX[1:180] to CBUF[91:270]. PE 3 copies DMAX[1:270] to CBUF[1:270]. In the first call of Sendrecv PE 0 sends its CBUF[1:270] to PE 1 and receives CBUF[1:270] of PE 3 onto its RBUF[1:270] and so on. The components of the order parameter x_i that yield the maximum distance along an angular bin and are stored in the array XMAX are communicated similarly. Then each PE compares its DMAX and RMAX and selects the maximum. For example, PE 0 compares DMAX[1:90] against RBUF[1:90] which contains what was in DMAX[1:90] of PE 3. PE 1 compares DMAX[91:180] against RBUF[1:90] which contains what was in DMAX[91:180] of PE 0, and so on. If a particular element of RBUF is selected, then it is copied onto the corresponding position of the array DMAX and the corresponding elements of XRMAX are copied onto XMAX also. Then each PE copies RBUF[91:270] onto CBUF[1:180] and XRMAX onto XCMAX similarly. In the second call of Sendrecv PE 0 sends its CBUF[1:180] to PE 1 and receives CBUF[1:180] of PE 3 onto its RBUF[1:180] and so on. Then PE 0 compares DMAX[1:90] against RBUF[1:90] which contains what was in DMAX[1:90] of PE 2. After $(N_p - 1)$ communications all processors finish updating their regions of DMAX.

Then each PE's updated region of DMAX must be sent to all other PEs. The array XMAX need not be communicated this time. Fortunately most distributed memory parallel machines have a convenient utility routine Concat which concatenates distributed data onto a larger array, as illustrated in [32]. In Paragon the routine is called 'Gcolx'. By calling Gcolx all PEs contribute and get the same copy of updated DMAX.

Table 6
Measurements of the computation τ_p and communication τ_m times in seconds with different number of PEs N_p; the computation was done on a Intel Paragon XP/S-15

N_p	τ_p(A)	τ_m(A)	γ(A)	S	τ_p(B)	τ_m(B)	γ(B)	S
5	0.5889	0.2180	0.37	3.65	5.0986	0.4213	0.08	4.62
10	0.3004	0.4126	1.37	4.13	2.6418	1.1998	0.45	6.66
15	0.2016	0.6348	3.15	3.52	1.6529	2.1395	1.29	6.72
20	0.1542	0.8548	5.54	2.92	1.2528	2.4693	1.97	6.85
30	0.1022	1.2683	12.4	2.15	0.8060	4.8614	6.03	4.50
40	0.0765	1.7167	22.4	1.64	0.6006	6.6102	11.0	3.54
60	0.0547	2.6076	47.7	1.11	0.4044	7.5329	18.6	3.21

This parallel algorithm is not exactly the same as the sequential version but the two versions need not be the same to achieve the goal of finding the orbit space boundary. As a matter of fact it is more natural that random walkers move in parallel exchanging information once in a while. Nor we have to use a parallel random number generator except at the beginning of the program to compute initial random points.

8.3. Test results

We have tested our algorithm on a Intel Paragon XP/S-15. We obtained the orbit spaces similar to Fig. 1 and Fig. 2. In addition we have measured the communication time τ_m and the computation time τ_p with different numbers N_p of PEs. The results are tabulated in Table 6. Convenient quantities [32] to measure the efficiency are the speedup $S(N_p) \equiv \tau_p(1)/(\tau_p(N_p) + \tau_m(N_p))$ and the efficiency $\epsilon \equiv S/N_p$. In the ideal case of zero communication time we should have $S(N_p) = N_p$ or $\epsilon = 1$.

Case A takes about 3 seconds in a uniprocessor machine. As N_p is increased, the machine spends more time for communication than computation. The ratio of the communication vs computation times $\gamma \equiv \tau_m/\tau_p$ ranges from 0.37 to 47.7. But as long as the total time ($= \tau_p + \tau_m$) is less than the uniprocessor time or S is greater than 1, it is worth to use the parallel machine. When N_p is above 60 the total time exceeds the uniprocessor time. This high communication overhead is due to the fact that the problem size is too small for a parallel machine.

Case B takes about 25 seconds in a uniprocessor machine. At the same N_p the communication overhead is less severe than case A. Case B requires about 8∼9 times more computing power than case A but case B requires only about 2∼3 times more data communication than case A. Even though the overhead is 1860% at $N_p = 60$ the total time is only about 8 seconds, still less than a third of the uniprocessor time. Due to a larger problem size the efficiency is higher in this case.

9. Discussions

For a d-dimensional orbit space, the distance measure is defined in the same way, i.e., the distance from the random walker's position to the center of gravity. In three dimensions, if the whole range of the two angles, polar and azimuthal, are divided into 180 and 360 bins, then the number of bins alone is huge, 64800. A fast workstation or a parallel supercomputer can handle this much data easily.

The problem size can become large if either the dimension of the order parameter is large as in the Higgs problem or the dimension of the orbit space is large as in the He-3 case. When the problem size is huge, the arrays `XMAX`, `XRMAX`, and `XCMAX` become too large to fit within the memory capacity of a processing element. Each PE can only store its region of the arrays and then the communication strategy must be changed accordingly.

For even higher dimensions, uniform binning of the directions is out of the question. We will need an adaptive Monte Carlo method in this case. Namely, we allocate more random walkers in regions of interest, i.e., convex regions. However, cusps can be found easily with only a few bins.

The random walker has to pass many singular curves on its march towards the surface. These curves are orbits of submaximal little groups. They are on the boundary surface in the full orbit space and the Jacobian of the orbit parameters with respect to x_m vanishes along those curves [6]. In the projected orbit space parts of the curves are buried inside. If δ or ω is too small the random walker may get stuck at the curves and may not be able to cross these singular curves as it never gets out of a cusp. So a reasonably large number, $0.5 \sim 1.0$, must be chosen at the expense of the increased rejection rate.

In conclusion, we have devised a general, efficient and robust Monte Carlo algorithm for finding the symmetry breaking directions. The method can be widely used both for the Higgs potential and the Landau potential. Our algorithm is not only useful in the invariant potential problem but also applicable to a wide range of optimization problems.

Acknowledgements

We have benefited from discussions with Prof. Michel. We thank Samsung Advanced Institute of Technology for giving us access to the Intel Paragon. This work was funded by Pohang University of Science & Technology and École Polytechnique. One of us (Kim) would like to thank for the hospitality of LSI at École Polytechnique, where this work was initiated.

References

[1] L. Michel, L.A. Radicati, in: Symmetry Principles at High Energy, Proc. 5th Coral Gables Conf. (Benjamin, New York, 1968) p. 19; Ann. Phys. (NY) 66, 758 (1971) 758.
[2] R. Slansky, Phys. Rep. 79 (1981) 1.
[3] J.F. Annett, Adv. Phys. 39 (1990) 83;
M. Sigrist, K. Ueda, Rev. Mod. Phys. 63 (1991) 239.
[4] Yu. M. Gufan, Sov. Phys. Solid State 13 (1971) 175.
[5] M. Abud, G. Sartori, Ann. Phys. (NY) 150 (1983) 307.
[6] J.S. Kim, Nucl. Phys. B196 (1982) 285;
S. Frautschi, J.S. Kim, Nucl. Phys. B 196 (1982) 301.
[7] M.V. Jarić, Phys. Rev. Let. 48 (1982) 1641.
[8] J. Bescq, S. Meljanac, D. Pottinger, Nucl. Phys. B 292 (1987) 222.
[9] H.T. Stokes, D.M. Hatch, Isotropy Subgroups of the 230 Crystallographic Space Groups (World Scientific, Singapore, 1988).
[10] J.C. Tolédano, P. Tolédano, J. Phys. 41 (1980) 189.
[11] L.D. Landau, E.M. Lifshitz, Statistical Physics, Part 1, §83 (Pergamon, Oxford, 1980).
[12] J.-I. Igusa, private communication (1984).
[13] L. Michel, in: Scientific Highlights in Memory of Léon Van Hove, F. Nicodemi, ed. (World Scientific, Singapore, 1993) p. 81; C.R. Acad. Sci. Paris 322, Series IIb (1995) 101.
[14] G. Barton and M.A. Moore, J. Phys. C 7 (1974) 4220.
[15] J.S. Kim, J.C. Tolédano, P. Tolédano, LANL cond-mat/9708084, unpublished.
[16] R.B. Jones, J. Phys. C 10 (1977) 657.
[17] C. Bruder, D. Vollhardt, Phys. Rev. B 34 (1986) 131.
[18] C.J. Cummins, R.C. King, J. Phys. A 19 (1986) 161.
[19] J.C. Tolédano, P. Tolédano, Landau Theory of Phase Transitions (World Scientific, Singapore, 1987).
[20] J.S. Kim, Group theoretical methods in spontaneous symmetry breaking, in: Selected Topics in Theoretical Physics, H.S. Song, ed. (Kyohak Sa, Seoul, 1986) pp. 192–225.
[21] J.S. Kim, Phys. Rev. B 31 (1985) 1433;
J.S. Kim, D.M. Hatch, H.T. Stokes, Phys. Rev. B 33 (1986) 1774.
[22] D. Hilbert, Math. Ann. 36 (1890) 473; 42 (1893) 313.

[23] J.S. Kim, L. Michel, B. Zhilinskii, Physical implications of crystal symmetry and time reversal. I The algebra of invariant real functions on the Brillouin zone, work in progress.
[24] J.S. Kim, J. Math. Phys. 25 (1984) 1694.
[25] J.S. Kim, C.W. Kim, Nucl. Phys. B 244 (1984) 523.
[26] B. Allen, Ann. Phys. (NY) 161 (1985) 152.
[27] M.V. Jarić, Phys. Rev. Let. 51 (1983) 2073.
[28] M. Abud, G. Anastaze, P. Eckert, H. Ruegg, Phys. Lett. B 142 (1984) 371.
[29] J. von Neumann, in: Monte Carlo Methods, G.E. Forsythe, H.H. Germond, A.S. Householder, eds., NBS Appl. Math. Series 12 (1951) 36.
[30] C.C. Tsuei et al., Science 271 (1996) 329.
[31] H. Georgi and S.L. Glashow, Phys. Rev. Lett. 32 (1974) 438.
[32] G.C. Fox et al., Solving Problems on Concurrent Processors (Prentice-Hall, Englewood Cliffs, NJ, 1988).

TEST RUN OUTPUT

The main result is output to a file "orb.s" which contains (x, y) data of the orbit space boundary. The terminal output is only for reporting program status, which starts after 5 Monte Carlo sweeps over angular bins.

```
--------------- Terminal Output --------------

Sweep count:  6  Deviation: 0.122950
Sweep count:  7  Deviation: 0.000076
Sweep count:  8  Deviation: 0.000088
Sweep count:  9  Deviation: 0.000024
Sweep count: 10  Deviation: 0.000043
Sweep count: 11  Deviation: 0.000033
Sweep count: 12  Deviation: 0.000037
Sweep count: 13  Deviation: 0.000025
Sweep count: 14  Deviation: 0.000024
Sweep count: 15  Deviation: 0.000015
Sweep count: 16  Deviation: 0.000024
Sweep count: 17  Deviation: 0.000007
 MC sweep count =  17
Dpts: 360  Delta:  0.25  Omega:  0.35
Success Rate:  0.248007   Deviation:  0.000007

----------  Some lines from "orb.s" ----------

    0.581148    0.581225
    0.585171    0.585205
    0.589256    0.589345
    0.593604    0.593635
    0.597895    0.598103
    0.602456    0.602732
    0.607385    0.607435
    0.612252    0.612657
    0.617990    0.618062
    0.623536    0.623621
    0.629282    0.629467
```